Title No. 121-S63

Seismic Effect of Reinforcement around Circular Opening in Reinforced Concrete Beam

by Koshiro Nishimura and Sujan Pradhan

In this study, five reinforced concrete (RC) beam specimens with transverse web openings and one specimen without openings were prepared. Diagonal steel bars were arranged around the web openings in the beam specimens so as not to fail at the section with the openings. The specimens were subjected to static reversed-cyclic shear loading of double curvature, and those specimens failed in shear at a different part than the section with the web openings.

This paper provides a simple model of the relationship between stress in the diagonal reinforcement around the openings and the applied shear load considering the shrinkage of concrete. Moreover, an evaluation method of the ultimate shear capacity of the beam using the upper-bound solution of the limit analysis was also provided. These models showed good agreement with the test results. The study contributes to the crack control and safety of RC beams with openings.

Keywords: crack control; opening; reinforced concrete (RC) beam; shear capacity; upper-bound theorem.

INTRODUCTION

Transverse web openings are often provided in beams of reinforced concrete (RC) buildings for plumbing utility ducts and pipes. ACI 318-19[1] requires that designers consider the effect of openings when calculating the shear strength of the beams at the section, but no specific methods are provided to calculate it. There are many openings of different shapes and sizes, which affect the behaviors and strength of the beams. Mansur[2] reviewed the previous study from the late 1960s to the 1990s on the behavior and design of RC beams with web openings subjected to bending and shear, classified those behaviors into beam-type and frame-type failures, and proposed the calculation methods of shear capacity for those types of failure. Further, Tan and Mansur[3] presented design guidelines for RC beams with large web openings. After that, Tan et al.[4] verified the calculation method with test data of RC beams with circular openings. There are many studies on the effect of transverse web openings in RC beams, such as RC deep beams with openings[5,6] and slender RC beams with multiple openings.[7] However, as Herrera et al.[8] pointed out, studies on RC beams with openings subjected to cyclic combined bending and shear are limited. In Japan, RC frame buildings are usually designed as seismic moment frames because earthquakes often occur; thus, transverse openings in RC beams are relatively small, and there is major interest in the behavior of the beams under reversed-cyclic loading. This paper discusses the influence of relatively small circular openings in RC beams subjected to cyclic combined bending and shear loads.

When designers examine the structural performance of RC buildings in Japan, they follow the "AIJ Standard for Structural Calculation of Reinforced Concrete Structures"[9] provided by the Architectural Institute of Japan (hereafter AIJ Standard). The AIJ Standard provides allowable and ultimate shear capacity equations for RC beams with circular and rectangular openings and requires that the height of the opening does not exceed one-third of the beam height. In addition, the AIJ Standard prohibits placing the web openings in plastic hinge regions as the regions are prone to damage due to the flexural yielding of the beam. The plastic hinges are usually assumed at the beam end regions in seismic designs. There are functional needs for constructing the openings at the end region of foundation beams designed not to yield in flexure under large earthquakes. In this study, providing an opening at the beam end region is one of the test parameters. Six beam specimens were prepared and subjected to static bending and shear loads of double curvature. To investigate the influence of web openings on the shear capacity in the section without openings in the beam, specimens were designed so as not to fail in the section with the openings based on the examination of calculated shear capacities. This paper discusses the test results of crack control around the web openings and the evaluation of ultimate shear capacities.

RESEARCH SIGNIFICANCE

In practical designs, a section around a web opening is reinforced with steel bars to avoid being weaker than sections without openings in the RC beam. This paper provides a method to evaluate the ultimate shear capacity around web openings, which is useful for examining the influence of openings on the shear. Moreover, this paper shows a model of relationships between tensile stress in the diagonal steel bars and shear force in the beam subjected to cyclic bending and shear loads of double curvature, which can be implemented to crack control.

EXPERIMENTAL PROGRAM
Specimen and loading setup

Five RC beam specimens with openings and one specimen without openings were prepared for the experimental study. Although the experimental program and results have been reported briefly,[10,11] details of the program and the results were added for discussion in this paper.

Figure 1 shows the dimensions and arrangement of the reinforcement of the specimens. The six specimens had

identical cross sections of 300 x 500 mm (11.8 x 19.7 in.), the same clear span-depth ratio of the beam (3.5 [1750/500]), the same number of longitudinal bars, and the same spacing of transverse reinforcement. As shown in Fig. 1, the parameters in these experiments are the number, diameter, and location of the openings and the bar arrangement around the openings. No openings were placed in Specimen DB-0. One opening was placed in Specimens DB-1 and DB-1c, with a difference in their positions (Fig. 1(b) and (d)). Another opening was added to DB-2 on the other side from the position of DB-1 so that the two openings were placed symmetrically (Fig. 1(c)). The two openings at the potential yield hinge regions were placed by both beam ends in DB-2e and DB-3ce, and an opening at the center was added to DB-3ce. The potential yield hinge region was decided based on the distance of beam depth from the beam end, where the AIJ Standard[9] prohibits placing the opening in the region. The diameters of the openings were 114 mm (4.5 in.) in the potential yield hinge region and 165 mm (6.5 in.) in the other sections. Table 1 shows the mechanical properties of deformed steel bars. The concrete strength, f_{cm}, is shown in Table 2, along with the calculated results of shear capacity, which are explained later. As shown in Table 2, the concrete strength of DB-0, DB-1, and DB-2 was somewhat lower than that of DB-1c, DB-2e, and DB-3ce as the concrete batches were different; however, the concrete mixture proportions were kept the same.

Figure 2 shows a photo of the loading setup. All the specimens were statically subjected to reversed-cyclic shear loading of double curvature, as shown in Fig. 3. The deformation angle and elongation of the beam were measured by the measurement system shown in Fig. 3, where two sets of the system were placed on both sides of the specimen. Cracks on the beam surfaces were sketched at the turning-back point of the load. Strains in the steel bars were measured with strain gauges, as shown in Fig. 1.

Structural properties of specimens

As shown in Fig. 1, both tensile and compressive longitudinal bars were arranged in double layers. The spacing of transverse reinforcement was decided based on the ratio ρ_t, to be approximately 0.3% so that shear failure would occur before the flexural failure of the specimens. The calculated capacities of all the specimens are shown in Table 2. When the specimens were designed, the shear capacities were calculated using equations provided by the AIJ Standard.[9] First, the shear capacities according to ACI 318-19, V_n in Table 2, are shown to understand the structural properties of specimens. Then, the shear capacity, V_{su}, is explained to show how the specimens were designed.

The shear capacity, V_n, is calculated according to Eq. (22.5.1.1) in ACI 318-19[1] as follows

$$V_n = V_c + V_s \qquad (1)$$

where V_c and V_s are the shear contributions of concrete and hoops, respectively, and Eq. (b) in Table 22.5.5.1 and Eq. (22.5.8.5.3) in ACI 318-19 are used for V_c and V_s when the capacity of the section without openings is calculated.

On the other hand, Mansur[2] suggested the simple expression of the shear capacity for the beam with openings by modifying V_n of ACI 318-19, and the same was adopted in this paper, as follows

$$V_c = 0.66\lambda(\rho_w)^{1/3}\sqrt{f_c'}\,b_w(d - d_o) \text{ (MPa)} \qquad (2)$$

$$V_s = \frac{A_v f_{yt}}{s}(d_v - d_o) + A_d f_{yd}\sin\alpha \qquad (3)$$

where λ is the modification factor for lightweight concrete (in this study, normal concrete was used, $\lambda = 1$); f_c' is the compressive strength of concrete; b_w is the web width; d is the distance from the extreme compression fiber to the longitudinal tension reinforcement; ρ_w is the ratio of the area of the longitudinal tension reinforcement to $b_w d$; s is the spacing of the transverse reinforcement; A_v is the area of the transverse reinforcement within the spacing s; A_d is the area of the diagonal reinforcement around the opening; f_{yt} and f_{yd} are the yield stresses of the transverse and diagonal reinforcement, respectively; d_v is the distance between the top and bottom longitudinal bars; d_o is the diameter of the web opening; and α is the angle of the diagonal reinforcement to the beam axis (refer to Fig. 4). Equation (2) is the same as Eq. (b) in Table 22.5.5.1 in the ACI 318-19 when the axial load and d_o are equal to zero, and Eq. (3) agrees with Eq. (22.5.8.5.3) when d is substituted for $(d_v - d_o)$ and A_d is equal to zero.

When the specimens were designed, the shear capacities were selected to be almost the same at the sections with and without openings according to the following equation provided by the AIJ Standard[9]

$$V_{su} = \left\{ \frac{0.156(\rho_w)^{0.23}(f_c' + 18)}{M/(Vd) + 0.12}\left(1 - 1.61\frac{d_o}{D}\right) + 0.85\sqrt{\sum\rho_s f_y} \right\} b_w\left(\frac{7d}{8}\right) \text{ (MPa)} \qquad (4)$$

$$\sum\rho_s f_y = \frac{A_{vc} f_{yt}}{b_w c} + \frac{A_{dc} f_{yd}}{b_w c}(\sin\alpha + \cos\alpha) \qquad (5)$$

where $M/(Vd)$ is the shear span ratio, where M is the largest bending moment in the beam; D is the overall depth of the beam; c is the distance shown in Fig. 4; and A_{vc} and A_{dc} are the areas of transverse and diagonal reinforcement within the region c, respectively. Equations (4) and (5) are the empirical equations based on the test results, where the influence of opening diameter was more significant than the lack of section due to the openings, so the contribution of concrete was reduced by 1.61 times d_o/D. The diagonal reinforcement was more effective than the transverse reinforcement, so $A_d f_{yd}$ was multiplied by $(\sin\alpha + \cos\alpha)$. Equation (4) agrees with the ultimate shear capacity equation without openings provided by the AIJ Standard,[9] which is referred to as the Arakawa formula in Japan.

As shown in Fig. 1, there are two types of arrangements of diagonal reinforcement for the specimens. One was a diamond shape with a development length formed by assembling four bent deformed bars of normal strength, which is the traditional way (refer to D-D' in Fig. 1(k)). Another was a closed diamond shape formed by bending a single deformed
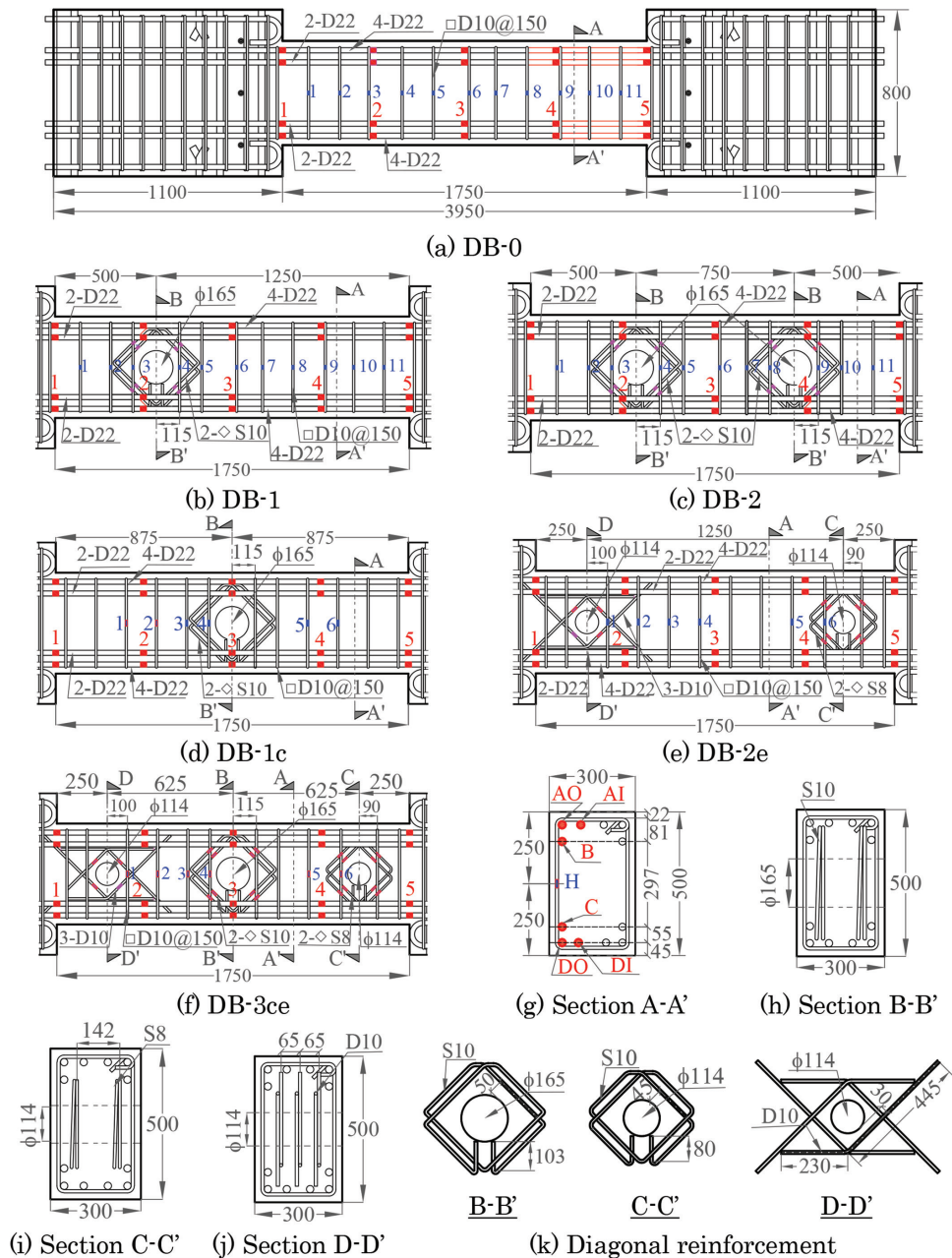
Fig. 1—Dimensions of specimens; north is to right in (a) to (f). (Note: Units in mm; 1 mm = 0.039 in.)

Table 1—Mechanical properties of deformed bars

Specimen	Designation	Grade	Nominal diameter, mm (in.)	Young's modulus, MPa	Yield stress, MPa	Tensile strength, MPa (psi)
DB-0, DB-1, and DB-2	D22	SD345	22.2 (0.87)	187,000	374	577 (83,700)
	D10	SD295	9.53 (0.38)	187,000	344	486 (70,500)
	S10	785	9.53 (0.38)	202,000	979*	1135 (165,000)
DB-1c, DB-2e, and DB-3ce	D22	SD345	22.2 (0.87)	190,000	368	593 (86,000)
	D10	SD295	9.53 (0.38)	188,000	351	498 (72,200)
	S10	785	9.53 (0.38)	197,000	975*	1146 (166,000)
	S8	785	7.94 (0.31)	208,000	1127*	1292 (187,000)

*0.2% offset method.

Note: Nominal cross-sectional areas are 387, 71, and 50 mm² for D22, D10 (or S10), and S8, respectively; 1 mm² = 0.00155 in.²; 1 MPa = 145 psi.

Table 2—Concrete strength and calculated results of shear capacity

Specimen	f_{cm}^*, MPa (psi)	V_f, kN	Section without opening		Section with opening of 165ϕ		Section with opening of 114ϕ	
			V_n, kN	V_{su}, kN	V_n, kN	V_{su}, kN	V_n, kN	V_{su}, kN
DB-0	28.3 (4100)	402	273	272	N/A			
DB-1					316	255	N/A	
DB-2					316	255		
DB-1c	34.9 (5060)	402	290	297	330	268	N/A	
DB-2e					N/A		310	282
DB-3ce					330	268	310	282

*Measured compressive strength of concrete cylinder.

Note: V_f is shear force at flexural yielding; V_n is shear capacity in accordance with ACI 318-19 or Mansur's equation; V_{su} is shear capacity in accordance with AIJ Standard; 1 kN = 0.225 kip.
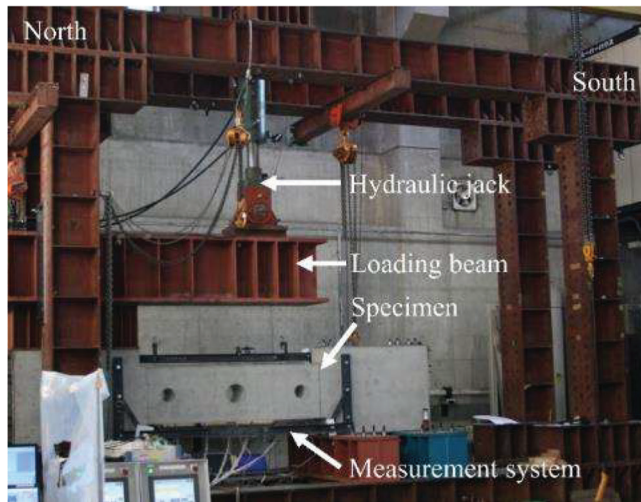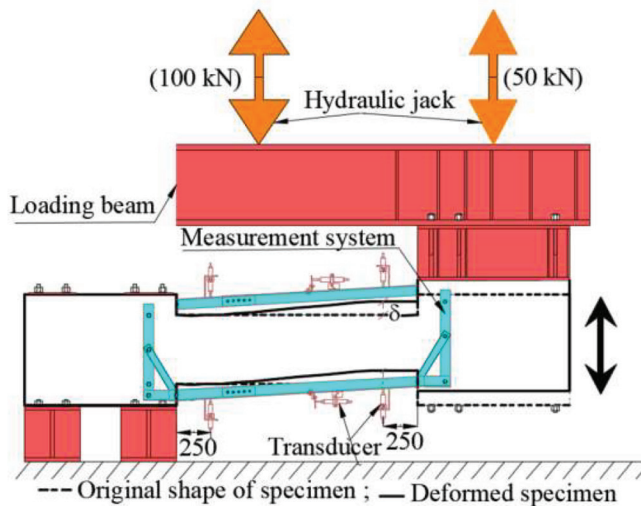

Fig. 2—Loading setup.

Fig. 3—Loading and measuring system. (Note: Units in mm; 1 mm = 0.039 in.)

Fig. 4—Reinforcement for opening shown in AIJ Standard.[9]

of the closed-shape reinforcement around the opening was decided as follows: the Grade SD295 deformed bars (refer to Table 1) were arranged in the traditional way (refer to Fig. 1(f)), and then ready-made, closed-shape reinforcement was replaced to have the same cross-sectional area as the traditional reinforcement. The ready-made reinforcement was a high-strength deformed bar, and it met the design policy of the specimens not failing at the web opening. It was confirmed that the stress in the closed-shape reinforcement did not significantly exceed the yield stress of SD295 in the tests, which is explained later. The values of shear capacities are calculated using the yield stress of SD295 shown in Table 1, though the closed-shape, high-strength reinforcement was used.

The calculated flexural capacity (V_f in Table 2) of six beam specimens is 402 kN (90.5 kip), which is the shear force when the bending moment at the beam ends reaches a yield bending moment; the strengths of concrete and deformed bars shown in Tables 1 and 2 are used in the calculation. The yield bending moment is calculated using the modified Kent-Park model[13] for the stress-strain curve of concrete and the elastic-perfectly plastic model for steel bars, where the longitudinal bar had a yield plateau, by increasing curvature until the strain at the extreme compression fiber of concrete reaches 0.003. As shown in Table 2, the V_n and V_{su} for the section without openings, which are almost the same, are lower than the V_f by approximately 30%. The shear capacities, V_{su}, with openings by the AIJ Standard are close to those without openings, as intended in the design (refer to Table 2). However, the specimens were expected to fail at the section without openings because V_n with openings was higher than that without openings; this means there was too much reinforcement around the web openings.

bar (refer to B-B' and C-C' in Fig. 1(k)). Because the specimens were scaled-down RC beams, the development length of the diagonal reinforcement in the traditional way was relatively long; thus, in the previous study,[12] the beam section without openings was over-strengthened against the design intention. Therefore, the closed diamond shape of reinforcement was mainly adopted in this study. The amount
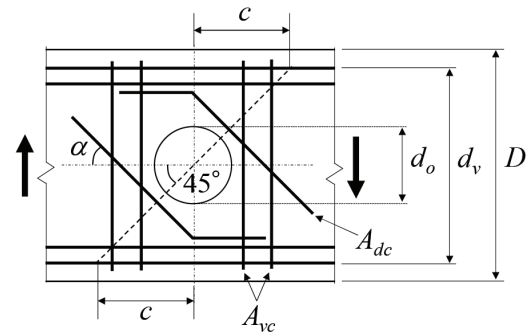
TEST RESULTS

Outlines of test results

Figure 5 shows the shear force and deformation angle relationship of the specimens, along with the relevant points and the evaluated shear capacities based on ACI 318-19,[1] V_n, and the AIJ Standard,[9] V_{su}, of the section without openings in Table 2. The load was first controlled with shear forces, where the load direction was turned back to allowable shear forces provided by the AIJ Standard[9] for both beams without and with openings (refer to Appendix A[*]). The allowable shear force has been adopted to moderate earthquakes with a return period of a few decades in practical design. Next, the load was controlled with a displacement of the beam stub (refer to Fig. 3), where the deformation angles R, which is the displacement divided by the clear span of the beam,

_____

of 0.005 and 0.01 rad were the turning-back points in both positive and negative directions. The positive direction of loading is downward displacement for Specimens DB-1 and DB-2 and is upward displacement for the other four specimens (refer to Fig. 3 and Appendix A). The shear load and deformation angle at each event are shown in Table 3; the calculated shear capacities in the table are explained later.

The shear force and deformation angle relationship of all specimens is almost the same up to the loading cycle of $R = 0.005$ rad regardless of the presence/absence, numbers, and location of the openings, which could be attributed to enough of the reinforcement around the openings. Furthermore, all specimens attributed the maximum load at the same loading cycle of deformation angle $R = 0.01$ rad to the beginning of degradation of the beam or to the following cyclic load, which had caused the failure. Specimen DB-3ce, with the largest number of openings, exhibited the highest capacity at a lower deformation angle (refer to Table 3) than the other specimens without showing the influence of the openings.
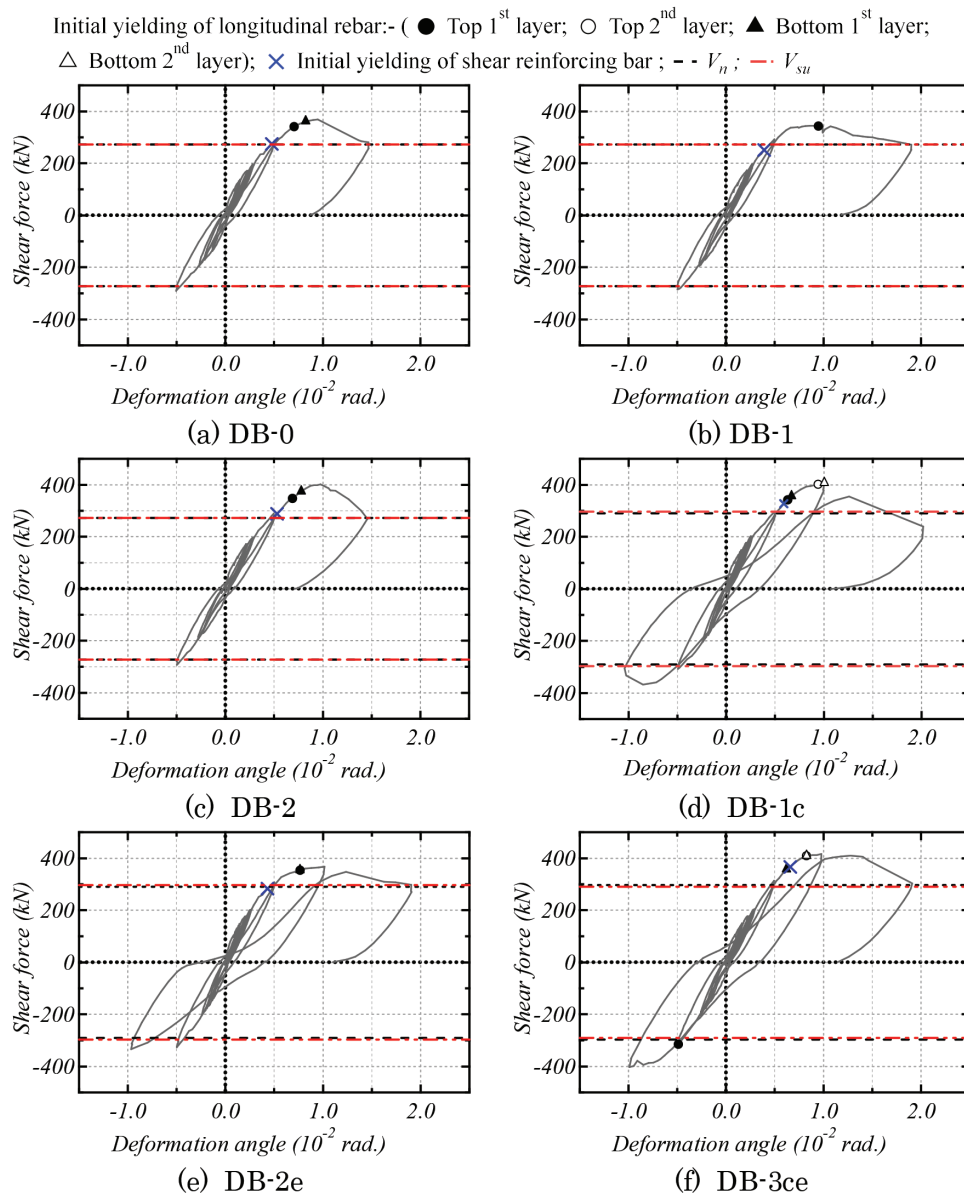

Fig. 5—Shear force and deformation angle relationship. (Note: 1 kN = 0.225 kip.)

Table 3—Shear load at events and shear capacity calculated by proposed model

Specimen	Initial yielding in outer (first) steel bar		Initial yielding in inner (second) steel bar		Maximum load in positive direction V_{u_exp}	Shear capacity calculated by Eq. (16) V_{u_cal}
	Positive direction	Negative direction	Positive direction	Negative direction		
DB-0	**342**; 7.1×10^{-3}	N/A	N/A	N/A	**368**; 9.5×10^{-3}	379
DB-1	**343**; 9.5×10^{-3}	N/A	N/A	N/A	**344**; 9.0×10^{-3}	379
DB-2	**348**; 6.9×10^{-3}	N/A	N/A	N/A	**401**; 9.8×10^{-3}	409
DB-1c	**343**; 6.3×10^{-3}	**−322**; -5.8×10^{-3}	**402**; 9.4×10^{-3}	N/A	**407**; 1.0×10^{-2}	420
DB-2e	**360**; 6.2×10^{-3}	**−324**; -6.9×10^{-3}	N/A	N/A	**368**; 7.7×10^{-3}	407
DB-3ce	**342**; 5.8×10^{-3}	**−315**; -4.9×10^{-3}	**409**; 8.3×10^{-3}	**−378**; -5.5×10^{-3}	**416**; 7.0×10^{-3}	423

Note: Boldface value is shear load in kN (1 kN = 0.225 kip); second value is deformation angle in radians; for instance, experimentally, maximum load is 368 kN and deformation angle is 9.5×10^{-3} rad for Specimen DB-0.

The capacity could have been attributed to the concrete compression strut inclination, which represents a path for shear force transformation due to the openings. Although shear capacity is discussed later, detailed studies are required to investigate the effect of openings on the stiffness in future. The longitudinal bars on the first layer of all the specimens yielded, except for Specimen DB-1 (only yielded on the top first layer); the reinforcing bars of Specimens DB-1c and DB-3ce, with the opening of 165 mm at the center, yielded on both layers. As shown in Fig. 5, the initial yielding of transverse reinforcement for all the specimens occurred around a deformation angle of $R = 0.005$ rad; in contrast, for Specimens DB-1c and DB-3ce, it occurred slightly later, when the deformation angle exceeded 0.005 rad. The initial yielding of the transverse reinforcement occurred prior to the initial yielding of longitudinal bars as per the design, as explained in the section "Structural properties of specimens."

Failure type and shear capacity

As shown in Fig. 5, all the specimens recorded higher shear capacities than the evaluated capacities, according to ACI 318-19[1] and the AIJ Standard,[9] of the sections without openings in Table 2. The ratio of the maximum experimental shear capacity, V_{u_exp}, to V_n from ACI 318-19 and V_{su} from the AIJ Standard of the section without openings was evaluated. The lowest ratio among all the specimens was 1.26/1.26 for Specimen DB-1 (with one opening) and 1.27/1.24 for Specimen DB-2e (with two openings of 114 mm (4.5 in.) at the beam end regions). On the other hand, the highest ratio was 1.47 for Specimen DB-2, with two openings of 165 mm (6.5 in.) at a symmetric position. Furthermore, it was 1.35, between the highest and lowest ratio, for Specimen DB-0 without any opening. Flexural cracks appeared on all the specimens during the first loading cycle. Figure 6 shows the cracks that appeared at the ultimate crack-recording deformation angle of $R = 0.005$ rad and the damage pattern on the specimens after the failure. As shown in Fig. 6, wide diagonal cracks extending from the edge of the north end toward the center span of the beam developed in all specimens except specimen DB-1c, which had an opening at the center, and concentrated cracks appeared near the opening. All the specimens failed in shear at the section without openings, though the longitudinal bars yielded on both layers in Specimens DB-1c and DB-3ce (refer to Table 3); thus, the shear capacity of these two specimens could be experimentally close to the flexural capacity. As a result, the shear force

of all the specimens degraded below 80% of the maximum force in the successive deformation angle without exceeding 0.02 rad (refer to Fig. 5).

EFFECT OF DIAGONAL REINFORCEMENT AROUND OPENING FOR CRACK CONTROL
Model for evaluating tensile stress in diagonal reinforcement

Mansur[2] recommended a sufficient amount of diagonal reinforcement for crack control for a small opening, and then Tan and Mansur[3] examined the contributions of the diagonal reinforcement based on the test results, where the amount of the diagonal reinforcement was calculated using the applied shear load and the yield stress of diagonal bars. In this paper, a relationship between tensile stress in the diagonal reinforcement and the applied shear load is discussed because evaluating the tensile stress in the diagonal reinforcement is reasonable for controlling cracking from the web opening.

In this study, the diagonal reinforcement was additionally placed around the openings in the specimens, while the amount of transverse reinforcement was the same as the beam specimen without openings (refer to Fig. 1). The normal-strength bars were used for the hoops and the traditional diagonal reinforcement, and the closed-shape diagonal reinforcement was made of the high-strength bar (refer to Table 1). Shear cracks occurred from the edge of the openings even if the shear load was relatively low, and then tensile strain in the diagonal reinforcement increased. To evaluate the tensile stress in diagonal reinforcement, simple shear stress-transfer models were proposed, as shown in Fig. 7, which shows cross sections without and with an opening. As shown in Fig. 7(a), a uniform shear stress, τ, is assumed on the cross section of the beam, and the same magnitude of shear stress occurs due to bond stress around the steel bars so that the stress field is a simple shear. Therefore, the tensile stress, σ, on the plane inclined at an angle of 45 degrees from the beam axis is equal to τ. As the cross section has a width of b_w and depth of d_v, the applied shear V is given as follows.

$$V = b_w d_v \tau \tag{6}$$

Figure 7(b) shows a model for a cross section with an opening of diameter d_o, where the diagonal reinforcement is placed in a direction at an angle of 45 degrees from the beam axis, and the diagonal reinforcement is at the right angle to
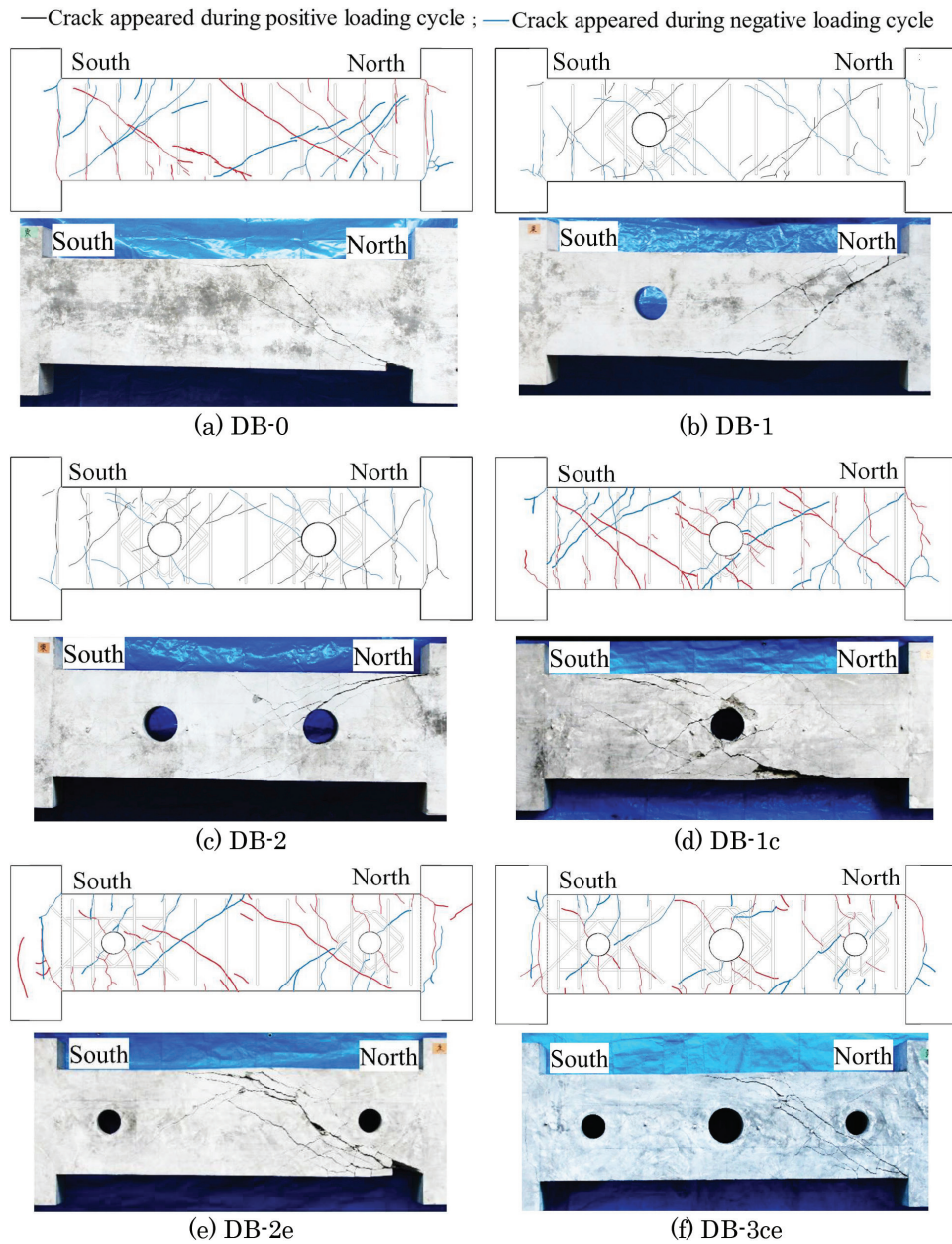
—Crack appeared during positive loading cycle ; —Crack appeared during negative loading cycle

(a) DB-0

(b) DB-1

(c) DB-2

(d) DB-1c

(e) DB-2e

(f) DB-3ce

Fig. 6—Sketch of observed cracks at R = 0.005 rad and photo after failure.

a diagonal crack. After diagonal cracking, a uniform tensile stress, σ, is assumed in concrete, the same as the section without openings, which is equal to τ, and tensile stress in the diagonal reinforcement, σ_d, is assumed to compensate for the lack of the tensile stress due to the web openings. Thus, the tension force of concrete, T_c, the tension force of the diagonal reinforcement, T_d, and the applied shear, V, can be given as follows.

$$T_c = \left(\frac{d_v}{\sin 45°} - d_o\right)b_w\sigma \tag{7}$$

$$T_d = \Sigma A_d\sigma_d \tag{8}$$

$$V = (T_c + T_d)\cos 45° \tag{9}$$

Equations (6) to (9) yield the following relationship because σ is equal to τ.

$$\Sigma A_d\sigma_d = \frac{d_o}{d_v}V \tag{10}$$

Figure 8 shows an idealized V-σ_d curve. The tensile stress in the diagonal reinforcement begins to increase after cracking (point A in Fig. 8). At this moment, the stress distribution in the concrete is not uniform. The stress in concrete is redistributed as the tensile stress σ_d increases, represented by the path from A to B in Fig. 8. After that, σ_d increases as V increases as per Eq. (10). If this behavior is valid, the required area of diagonal bars can be determined by V and σ_d like a service load, V_{serv}, and an allowable stress, σ_{serv}. However, the influence of such on the shrinkage of the concrete must be considered when this model is compared with the test results. Before loading the specimen, the diagonal reinforcement is in compression due to the shrinkage of the concrete; thus, the measured strain in the diagonal reinforcement is initialized in this condition. The strain in the diagonal reinforcement will be released when the diagonal
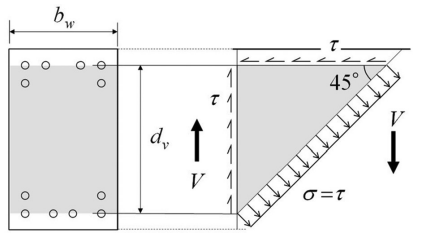
(a) Stresses in beam without opening
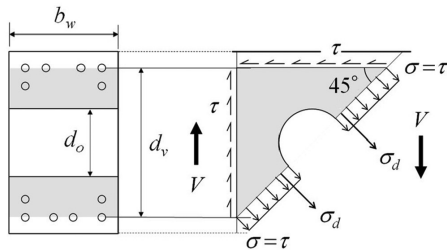
(b) Stresses in beam with opening

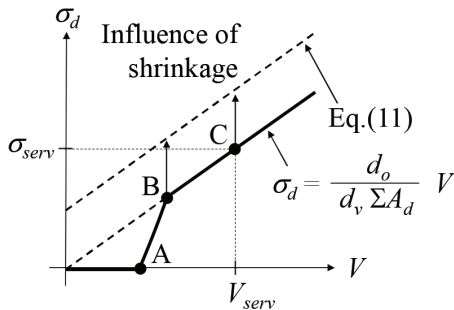*Fig. 7—Stress-transfer model of cross section in beam.*

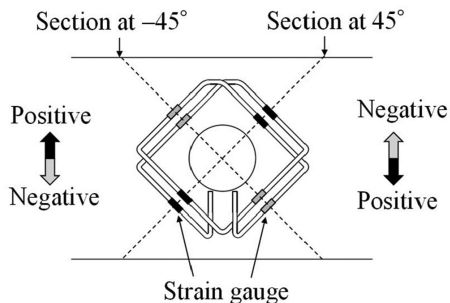*Fig. 8—Idealized* V-σ_d *relationship.*

Fig. 9—Location of strain gauges.

crack occurs. This behavior makes σ_d increase so that the path from B to C in Fig. 8 shifts upward. Therefore, Eq. (10) yields the following equation

$$\sigma_d = \frac{d_o}{d_v\sum A_d}V + E_d\varepsilon_r \qquad (11)$$

where E_d is the Young's modulus of elasticity of the diagonal bar; and ε_r is the strain in the diagonal bar released from shrinkage by cracking in concrete. Equation (11) has been derived assuming that the ε_r is dominant, though other parameters would affect the initial strain in diagonal reinforcement.

Validation of model for crack control

Equation (11) is compared with the test results. Stress in the diagonal reinforcement is calculated by multiplying strain measured at the portion shown in Fig. 9 by the Young's modulus shown in Table 1. The dark and light gray solid curves in Fig. 10 are the relationships between the stress and the applied shear load divided by the maximum shear load, V_{u_exp}, of each specimen up to the deformation angle 0.005 rad. The stress of the dark gray line is the average of the stresses measured by the strain gauges of the dark gray marks in Fig. 9, which are at the intersection by a broken line of a 45-degree angle. The stress of the dark gray line will be positive as the positive shear is applied. On the other hand, the stress of the light gray line will be positive as the negative shear is applied, where the light gray line is given in the same manner as the dark gray one (refer to Fig. 9). The two broken lines in Fig. 10 are the calculated results using Eq. (11), where the absolute value of the shear load is substituted for V, and ε_r is assumed to be 0.0002.

The comparison in Fig. 10 revealed that the calculated results were approximately consistent with the unloading and reloading paths of the test results, particularly for specimens with a single opening. The stress in the traditional diagonal reinforcement is a little larger than the calculated results in Specimen DB-2e. It is considered to be due to the nonlinear behavior of the bar, though the bar did not yield at the point where the strain gauge was installed; however, the bar might have yielded at the point where the strain was not monitored. In contrast, the calculated result had good agreement with Specimen DB-2. On the other hand, the stresses were a little larger than the broken lines for DB-3ce, which might be the influence of adjacent openings. Hence, the proposed model can be used to evaluate the residual stress after a seismic event; thus, the study contributes to the crack control of beams with openings. It should be noted that the value of 0.0002 for ε_r is a tentative value because the number of specimens used to validate the proposed models was limited to five, and it is not easy to estimate the ε_r in practical design. Moreover, factors other than the concrete shrinkage could affect the initial strain in diagonal reinforcement and might make it necessary to revise Eq. (11). Hence, further studies are required to reinforce/validate the proposed model.

EVALUATION OF SHEAR CAPACITY
Upper-bound solution of shear capacity

In this study, the specimens failed in shear at the section without openings. The upper-bound solution of the limit analysis based on the plastic theory is used to evaluate the shear capacities and the failure location. Regarding the shear problem in RC beams without openings, Nielsen[14] showed the upper-bound solution. While Nielsen derived the shear capacity of an RC beam, replacing the force in the transverse reinforcement with a uniform equivalent stress, Ichinose and Yokoo[15] developed the upper-bound solutions considering the spacing of transverse reinforcement. This paper provides a solution for beams with openings, developing the model proposed by Ichinose and Yokoo.[15]

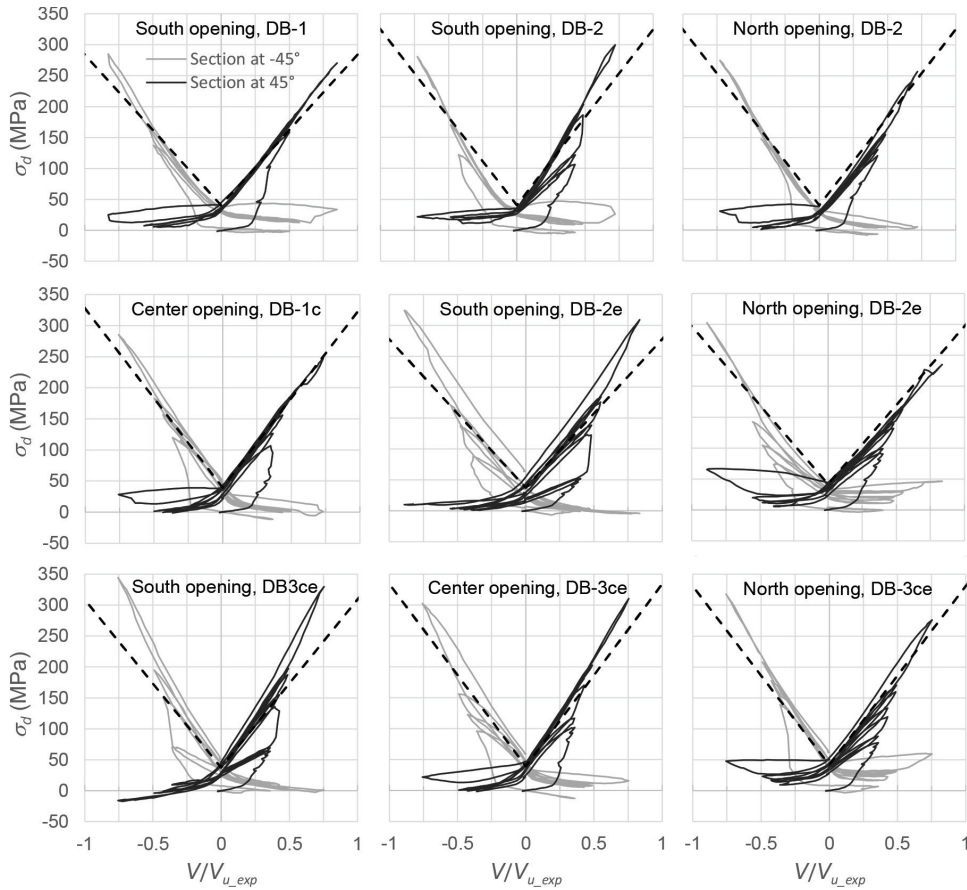Figure 11 shows an RC beam with evenly spaced transverse reinforcement. The effective cross-sectional area of the

Fig. 10—V-σ_d curves of test results up to deformation angle of 0.005 and Eq. (11) where ε_r = 0.0002. (Note: 1 MPa = 145 psi.)

beam is $b_e d_v$ as Ichinose and Yokoo[15] assumed the effective cross-sectional area neglecting the cover concrete because it no longer contributes to the ultimate condition due to cracks. The yield line at the angle of β and the virtual displacement of u are also illustrated. The dissipation per unit length in the concrete at the yield line, w_c, can be given assuming the plane stress and tensile strength for concrete are zero, as follows[14] (Appendix B)

$$w_c = \frac{1}{2}uf_c b_e(1 - \cos\beta) \qquad (12)$$

where b_e is the effective width; and f_c is the nominal compressive strength of concrete. The work equation gives the following relationship between the external work, Vu, and the internal works.[14]

$$V \cdot u = \frac{1 - \cos\beta}{2\sin\beta}uf_c b_e d_v + \frac{d_v\cot\beta}{s}uf_{yt}A_v \qquad (13)$$

The first term in Eq. (13) is the dissipation of concrete, multiplying the length of the yield line with w_c, and the second is the dissipation of the transverse reinforcement crossing the yield line. Because the first and second terms in Eq. (13) are decreasing and increasing functions with respect to the angle β, respectively, the minimum value of Eq. (13) with respect to β gives the upper-bound solution of the shear capacity of the RC beam[14] (Appendix B). The effective strength of the concrete is usually required to compensate for the gap between the theory and test results of
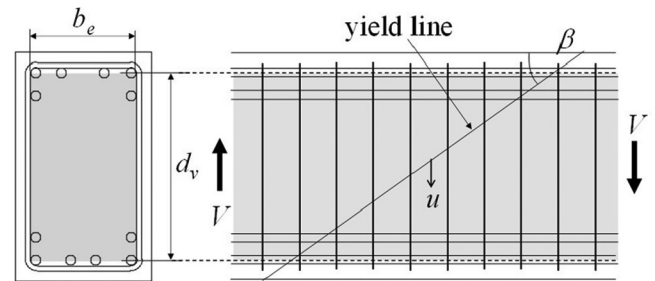

Fig. 11—Shear failure model of RC beam.

beam specimens. Nielsen[14] shows a conservative equation of the effective factor, ν, as follows.

$$f_c = \nu f_c' = \left(0.7 - \frac{f_c'}{200}\right)f_c' \text{ (MPa)} \qquad (14)$$

However, the spacing of transverse reinforcement may influence the shear capacity when the transverse reinforcement is not dense enough. Ichinose and Yokoo[15] analytically discussed this problem based on the upper-bound theorem and claimed that the spacing of transverse reinforcement may give lower shear capacity. Because the dissipation in the concrete given by the first term of Eq. (13) is a decreasing function with respect to the angle β, the lowest-angle β gives the upper-bound solution if the dissipation in the transverse reinforcement is a constant value. For example, as shown in Fig. 12, the dissipation in the transverse reinforcement is constant, as the number of the reinforcement intersecting the yield line,

n_v, is three when β is less than $β_2$ and greater than or equal to $β_3$; thus, when n_v is equal to three, the angle of $β_3$ gives the lowest value in Eq. (13). Therefore, the minimum value of the external works of every potential n_v is the solution.

Nielsen[14] and Ichinose and Yokoo[15] assumed the yield line to be straight because it gives a lower value than polygonal lines. In this paper, polygonal yield lines are considered in the beam with openings because the line that avoids the diagonal reinforcement may give a solution. Some examples of the polygonal yield lines are shown in Fig. 13. As Mansur[2] assumed a failure line to pass the center of the opening, the yield line passing the center of the opening is reasonable, as shown in Fig. 13(a), when the circular opening is relatively small, like the specimens in this study. In Fig. 13(b) to (d), the yield line is assumed to be bent at the intersection points of the diagonal reinforcement. The dissipation in the concrete can be obtained by adding the dissipation of the line segments of the polygonal yield line so that the equilibrium between the external and the internal works can be given as follows

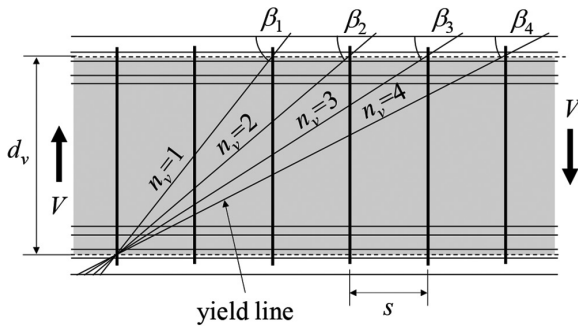$$V \cdot u = \sum_i (l_{yi} w_{ci}) + n_v A_v f_{yt} u + A_d f_{yd} u \sin\alpha \quad (15)$$

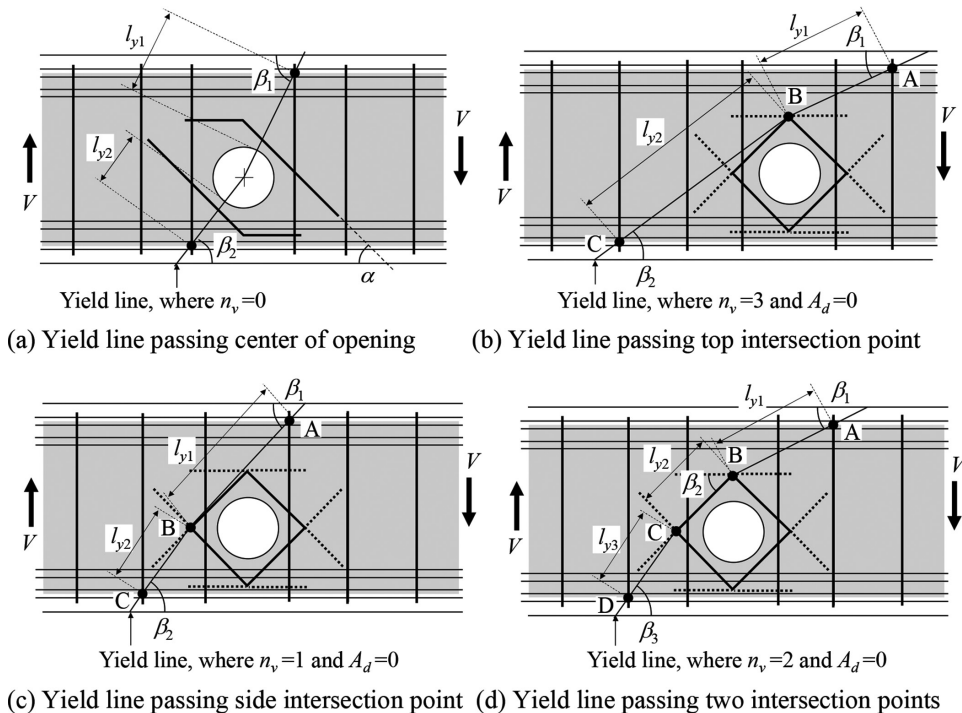Fig. 12—Shear failure model proposed by Ichinose and Yokoo.[15]

where i is the number of segments in the polygonal yield line; and the first, second, and third terms are the dissipations of the concrete, transverse reinforcement, and diagonal reinforcement, respectively. Substituting Eq. (12) and (14), Eq. (15) yields the following equation.

$$V = \sum_i \left\{ \frac{b_e v f_c'}{2} l_{yi} (1 - \cos\beta_i) \right\} + n_v A_v f_{yt} + A_d f_{yd} \sin\alpha \quad (16)$$

In the case of Fig. 13(a), the diagonal reinforcement is crossed by the yield line and is considered in the calculation using Eq. (16). When the yield lines avoid the diagonal reinforcement, as shown in Fig. 13(b) to (d), A_d in Eq. (16) is assumed to be zero. The upper-bound solution is given when the V, according to Eq. (16), is minimized among every potential yield line.

Shear capacities of specimens

The measured results of stress in hoops and diagonal reinforcement at the maximum positive load are shown in Fig. 14 (refer to Fig. 1 for the location of the strain gauges). The horizontal broken line in Fig. 14, f_y', is the yield stress of the normal-strength deformed bar used for the D10 hoops (refer to Table 1). The tensile stress in the closed-diamond-shaped reinforcement is the average value of the double bars on each side of the square shape. The yield lines giving the solutions in the six specimens are also shown in Fig. 14. As shown in Fig. 14(a), which is the result of Specimen DB-0 without openings, the yield line crossing three transverse bars ($n_v = 3$ in Eq. (16)) gives the solution. When the value of V is calculated by Eq. (16), the yield stress in Table 1 and the f_{cm} in Table 2 are substituted for f_{yt} and f_c', respectively, except for the diagonal reinforcement. Regarding the tensile stress in the diagonal reinforcement, because the high-strength reinforcement was used (refer to S8 and S10 in Table 1)

(a) Yield line passing center of opening

(b) Yield line passing top intersection point

(c) Yield line passing side intersection point

(d) Yield line passing two intersection points

Fig. 13—Potential yield line around opening.

and did not yield, the tensile stress at the maximum load is substituted for f_{yd}. As shown in Fig. 14, the stress in the diagonal reinforcement did not significantly exceed the f_y' of normal-strength reinforcement. Thus, when normal-strength steel bars are adopted for diagonal reinforcement in design applications, the nominal yield stress can be used. The shear forces V of the specimens with openings were calculated by Eq. (16), considering that a shallower angle of the yield line gives a lower value, and the number of hoops crossed by the yield line increases the value. As a result of the examination of every potential yield line, including lines extending to the beam end, as shown in Fig. 14, the shear forces given by the lines that did not cross the diagonal reinforcement were lower than those given by the yield lines that passed the opening. The specific examinations of deciding the solution among the potential yield lines are shown in Appendix C.

The yield lines are validated by the observed stress and cracks in the test. Figure 14(a) shows the result of Specimen DB-0 without openings, and the tensile stresses in the hoops intersected by the yield line reach the yield stress. The yield line agrees with the wide crack observed after the failure, shown in Fig. 6(a). The results of Specimens DB-1 and DB1c,

which have one opening with a diameter of 165 mm, are shown in Fig. 14(b) and (d), respectively. The wide cracks can be seen in Fig. 6(b) and (d) at the same location as the yield lines shown in Fig. 14(b) and (d). Regarding the results of Specimens DB-2, DB-2e, and DB-3ce, shown in Fig. 6 and 14, the wide cracks can also be seen at the same locations as the yield lines. As shown in Fig. 14, when the shear load was the maximum, although the tensile stresses in all the hoops at the yield line did not reach the yield stress, the stresses were relatively higher than those in the hoops at the other parts. The yield lines giving the solution are approximately valid as a result of comparison with the damage pattern in the test.

The minimum value in Eq. (16) among the potential yield lines is the calculated shear capacity, V_{u_cal}, and the results are shown in Table 3, where the V_{u_cal} is compared with the measured maximum load, V_{u_exp}. Figure 15 shows the comparison between the calculated results of all six specimens and the test values. The V_{u_cal} was mainly affected by the angle of the yield line and the concrete strength (refer to Table 2) because the yield lines in all six specimens crossed three hoops ($n_v = 3$ in Eq. (16)), as shown in Fig. 14. For instance, although DB-3ce had three openings and DB-1c
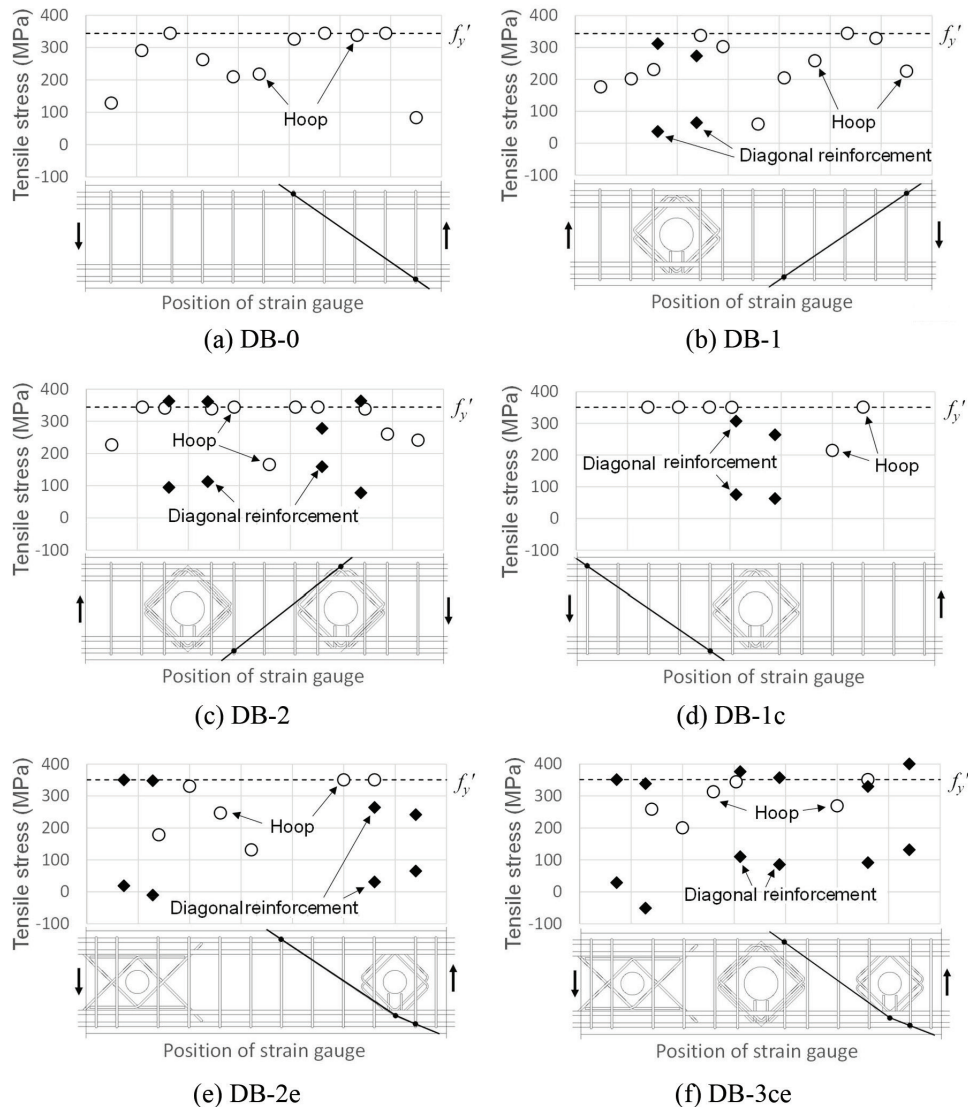

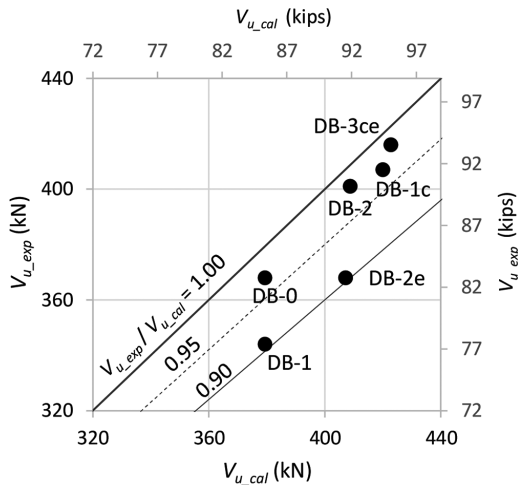Fig. 14—Expected yield line and stress in reinforcement. (Note: 1 MPa = 145 psi.)

Fig. 15—Comparison between test results and calculations of shear capacities.

had one, the test value of DB-3ce was higher than that of DB-1c, and the calculated results represent this difference because the angle of the yield line in DB-3ce is steeper than that in DB-1c. Similarly, the angle of the yield line in DB-2 is steeper than that in DB-0. The V_{u_exp}/V_{u_cal} ratios of these four specimens are almost the same: 0.97 or 0.98. However, the V_{u_exp}/V_{u_cal} of DB-1, which is 0.91, is less than that of DB-0, even though the angles of the yield lines and the concrete strengths were the same. The proposed method still has some scatters and somewhat overestimates the test results. The test parameters in this study are limited to proposing a recommendation for the diameter of the opening and its reinforcement. Hence, further studies are required, along with the verification of other existing test data, to improve the method and provide a design recommendation.

CONCLUSIONS

In this study, five reinforced concrete (RC) beam specimens with transverse web openings and one specimen without openings were prepared. Diagonal reinforcement was arranged around the web openings in beam specimens so as not to fail at the section with the openings. The specimens were subjected to static reversed-cyclic shear loading of double curvature, and those failed in shear at a different part than the section with the web openings.

This paper provided a simple model of the relationship between stress in the diagonal reinforcement around the openings and the applied shear load considering the shrinkage of the concrete, where it was assumed that the shrinkage is dominant, although other parameters would affect initial strain in the diagonal reinforcement. The model was validated by comparing the test results, which implies it can be useful for crack control by evaluating residual stress after an earthquake if strains due to shrinkage of the concrete can be estimated. However, factors other than the shrinkage could affect the initial strain in diagonal reinforcement. Hence, further studies are required to reinforce and validate the proposed model.

An evaluation method of the ultimate shear capacity of the beam using the upper-bound solution of the limit analysis was also provided. Polygonal yield lines were adopted to simulate the failure section in the specimens, and the spacing of the

reinforcement was considered in the method. As a result of the comparison between the test and calculated results, the location of the yield line was almost the same as the failure section of each specimen. The calculated values of shear capacities successfully represented differences in the maximum shear loads of specimens to a certain degree, though the method still has some scatters and somewhat overestimates the test results. Thus, further studies are required, along with the verification of other existing test data, to improve the method.

AUTHOR BIOS

*ACI member **Koshiro Nishimura** is an Associate Professor at Tokyo Institute of Technology, Tokyo, Japan, where he received his PhD in engineering. His research interests include the evaluation of the seismic performance of building structures.*

***Sujan Pradhan** is an Assistant Professor at Tokyo Institute of Technology. He received his PhD in engineering from Osaka University, Osaka, Japan.*

REFERENCES

1. ACI Committee 318, "Building Code Requirements for Structural Concrete (ACI 318-19) and Commentary (ACI 318R-19) (Reapproved 2022)," American Concrete Institute, Farmington Hills, MI, 2019, 624 pp.

2. Mansur, M. A., "Effect of Openings on the Behaviour and Strength of R/C Beams in Shear," *Cement and Concrete Composites*, V. 20, No. 6, 1998, pp. 477-486. doi: 10.1016/S0958-9465(98)00030-4

3. Tan, K.-H., and Mansur, M. A., "Design Procedure for Reinforced Concrete Beams with Large Web Openings," *ACI Structural Journal*, V. 93, No. 4, July-Aug. 1996, pp. 404-411.

4. Tan, K.-H.; Mansur, M. A.; and Wei, W., "Design of Reinforced Concrete Beams with Circular Openings," *ACI Structural Journal*, V. 98, No. 3, May-June 2001, pp. 407-415.

5. Yang, K.-H., and Ashour, A. F., "Effectiveness of Web Reinforcement around Openings in Continuous Concrete Deep Beams," *ACI Structural Journal*, V. 105, No. 4, July-Aug. 2008, pp. 414-424.

6. Tseng, C.-C.; Hwang, S.-J.; and Lu, W.-Y., "Shear Strength Prediction of Reinforced Concrete Deep Beams with Web Openings," *ACI Structural Journal*, V. 114, No. 6, Nov.-Dec. 2017, pp. 1569-1579. doi: 10.14359/51700950

7. Aykac, B.; Aykac, S.; Kalkan, I.; Dundar, B.; and Can, H., "Flexural Behavior and Strength of Reinforced Concrete Beams with Multiple Transverse Openings," *ACI Structural Journal*, V. 111, No. 2, Mar.-Apr. 2014, pp. 267-278.

8. Herrera, L.; Anacleto-Lupianez, S.; and Lemnitzer, A., "Experimental Performance of RC Moment Frame Beams with Rectangular Openings," *Engineering Structures*, V. 152, Dec. 2017, pp. 149-167. doi: 10.1016/j.engstruct.2017.08.043

9. AIJ, "AIJ Standard for Structural Calculation of Reinforced Concrete Structures," Architectural Institute of Japan, Tokyo, Japan, 2018. (in Japanese)

10. Zheng, J.; Kyunai, Y.; Hara, K.; Sugihara, K.; and Nishimura, K., "Experimental Study on RC Foundation Beam with Openings in Beam End Region, Part 1 Experimental Program, Part 2 Test Results," *Summaries of Technical Papers of Annual Meeting*, Architectural Institute of Japan, Structure IV, 2021, pp. 301-304. (in Japanese)

11. Zheng, J.; Takahashi, N.; and Nishimura, K., "Experimental Study on Influence of Location of Openings in RC Beam on Shear Capacity, Part 1 Experimental Program and Results, Part 2 Effect of Opening at Beam End," *Summaries of Technical Papers of Annual Meeting*, Architectural Institute of Japan, Structure IV, 2022, pp. 253-256. (in Japanese)

12. Shibao, K., and Nishimura, K., "Experimental Study on Structural Performance of RC Beam with Opening and Longitudinal Cut Off Bars," *Journal of Structural and Construction Engineering (Transactions of AIJ)*, V. 86, No. 785, 2021, pp. 1095-1105. (in Japanese)

13. Park, R.; Priestley, M. J. N.; and Gill, W. D., "Ductility of Square-Confined Concrete Columns," *Journal of the Structural Division*, ASCE, V. 108, No. 4, Apr. 1982, pp. 929-950. doi: 10.1061/JSDEAG.0005933

14. Nielsen, M. P., *Limit Analysis and Concrete Plasticity*, second edition, CRC Press, Boca Raton, FL, 1998, 908 pp.

15. Ichinose, T., and Yokoo, S., "Effects of Sparseness of Shear Reinforcement on Shear Strength of R/C Beam," *Journal of Structural and Construction Engineering (Transactions of AIJ)*, V. 437, July 1992, pp. 97-103. (in Japanese)
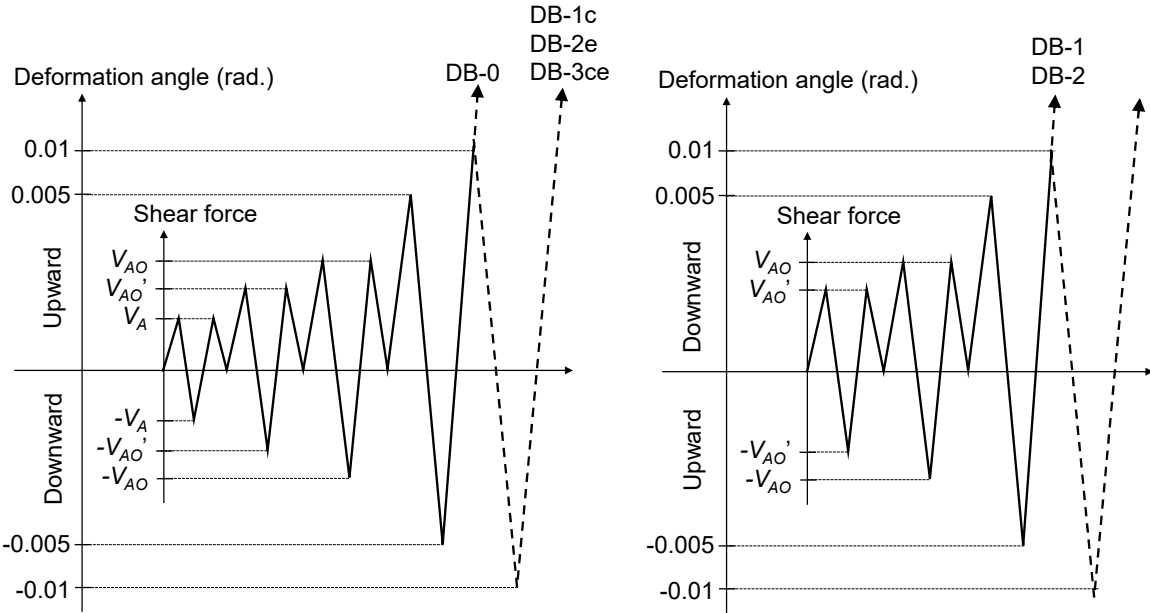
APPENDIX A

Loading protocol

Loading protocols are shown in Fig. A1. All the specimens were statically subjected to cyclic reversal shear load of double curvature as shown in Fig.3. The positive direction of loading is downward displacement for the specimens DB-1 and DB-2 (Fig. A1b) and is upward displacement for the other four specimens (Fig. A1a). The load was first controlled with shear forces where allowable shear forces provided by the AIJ Standard[9] were the turning back points in both positive and negative directions. The allowable shear capacity for a beam can be calculated by the following equation[9].

$$V_{AO} = \left\{ \xi f_s \left(1 - \kappa \frac{d_o}{D} \right) + 0.5 f_{wt} (\rho_s - 0.002) \right\} b_w \left(\frac{7d}{8} \right) \quad \text{(MPa)} \qquad \text{(A1)}$$

In the above equations, ξ is the increasing factor in the range from 1 to 2 as the shear span ratio decreases; f_s is the allowable shear stress of concrete; κ is the reduction factor for the diameter of opening; f_{wt} is the allowable tensile stress of the reinforcement, and the other symbols are the same as Eq. 4. Equation A1 is the simplified formula of Eq. 4 with a margin. The first turning back point in Fig. A1a, V_A, is given by substituting zero for d_o in Eq. A1. The V_{AO} and V_{AO}' are given by substituting 1.00 and 1.61 for κ in Eq. A1, respectively. Next, the load was controlled with a displacement of the beam stub (see Fig. 3) where the deformation angles R, which is the displacement divided by the clear span of the beam, of 0.005 and 0.01 radian were the turning back points in both positive and negative directions.

(a) DB-0, DB-1c, DB-2e, and DB-3ce. (b) DB-1 and DB-2.

Fig. A1 – Loading protocol.

APPENDIX B

Upper bound solution of shear capacity of beam with transverse reinforcement

The shear capacity of a reinforced concrete (RC) beam with shear reinforcement is derived in the same manner as Nielsen[14]. Figure B1 shows an RC beam with evenly spaced transverse reinforcement. The yield line at the angle β is also illustrated. As the transverse reinforcement is spaced closely, the force in transverse reinforcement is replaced with a uniform equivalent stress. Figure B2 shows a volume at the yield line in the concrete bounded by two parallel planes with the distance of δ, and neglecting the cover concrete. When the two parts of the beam have the displacement of u, the strains in the volume can be given as follows.

$$\varepsilon_{xx} = 0 \tag{B1}$$

$$\varepsilon_{yy} = \frac{\Delta y}{\delta} = \frac{u \cos \beta}{\delta} \tag{B2}$$

$$\gamma_{xy} = \frac{\Delta x}{\delta} = \frac{u \sin \beta}{\delta} \tag{B3}$$

These strains translate into the maximum and the minimum principal strains, respectively as follows.

$$\varepsilon_1 = \frac{u}{2\delta}(\cos \beta + 1) \tag{B4}$$

$$\varepsilon_3 = \frac{u}{2\delta}(\cos \beta - 1) \tag{B5}$$

A yield condition of the concrete, which is the plane stress and the tensile strength of zero, is assumed as shown in Fig. B3. The yield surface is illustrated in a coordinate of the maximum and minimum principal stresses, σ_1 and σ_3, and the principal strain vector of Eqs. B4 and B5 are also inserted. In accordance with the associated flow rule of the plastic theory, the strain vector determines the stress point of $(\sigma_1, \sigma_3) = (0, -f_c)$. Therefore, the dissipation per unit length in the concrete at the yield line, w_c, can be given as follows where b_e is the width of the beam.

$$w_C = b_e \delta (\varepsilon_1 \sigma_1 + \varepsilon_3 \sigma_3) = \frac{1}{2} f_c u b_e (1 - \cos \beta) \tag{B6}$$

The following equation is the dissipation in the transverse reinforcement crossing the yield line,

$$W_S = \frac{A_v d_v \cot \beta}{s} f_{yt} u \tag{B7}$$

The work equation gives the following relationship between the external and internal works.

$$V \cdot u = \frac{d_v}{\sin \beta} w_C + W_S = u f_c b_e d_v \frac{1 - \cos \beta}{2 \sin \beta} + \frac{A_v d_v \cot \beta}{s} f_{yt} u \tag{B8}$$

When the shear force V is minimized with respect to the angle β, the upper bound solution can be given as follows.

3

$$V = b_e d_v f_c \sqrt{\Psi(1 - \Psi)} \qquad \text{(B9)}$$

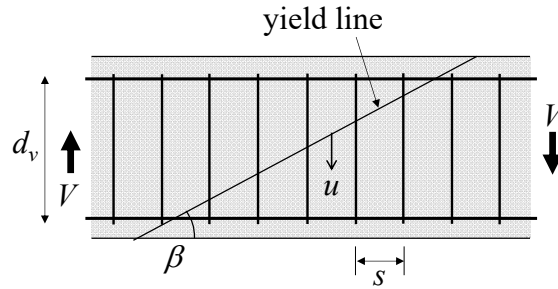$$\Psi = \frac{A_v f_{yt}}{b_e s f_c} \qquad \text{(B10)}$$

Fig. B1 – Shear failure model of RC beam
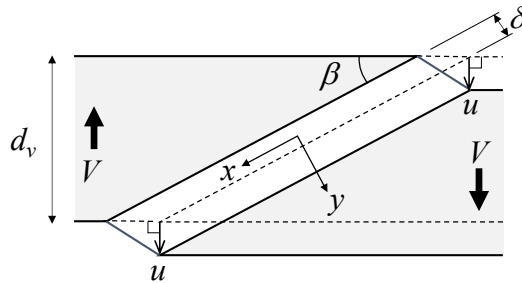

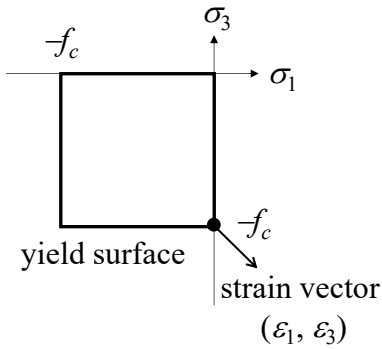*Fig. B2 – Strain field at yield line of concrete.*

Fig. B3 – Failure criterion of concrete.

4

APPENDIX C

Calculation of shear capacity using Eq. 16

Examinations of deciding the upper bound solution of shear capacity of the specimens are shown in detail. When the shear force V is calculated by Eq.16, the yield stress in Table 1, f_{cm} in Table 2, and the measured tensile stress in the diagonal reinforcement at the maximum load are substituted for the f_{yt}, f_c', and f_{yd}, respectively.

As shown in Fig. C1, the yield line crossing three hoops, $n_v=3$, gives the solution for the specimen DB-0 without opening because the shear forces given by the yield lines of $n_v=2$ and $n_v=4$ are larger than it where the n_v is the number of sets of the transverse reinforcement intersected by the yield line.

In case of the specimen DB-1 shown in Fig. C2, V_{IJ} is the solution because the values around the opening are larger than it; the minimum value for the section around the opening is V_{EF} the yield line of which crosses eight diagonal reinforcing bars and $n_v=0$. Further, V_{AB} was larger than the V_{EF}; point A is the intersection of the diagonal reinforcing bars, where is almost the same as the place of the longitudinal bar in outer layer; point B is defined at the beam end.

Regarding the specimen DB-1c shown in Fig. C3, it was confirmed that the yield line of $n_v=3$ gives the lowest value V_{AB} for the part without opening though the concrete strength of DB-1c was a little higher than DB-0 and DB-1 (see Table 2). The shear forces of V_{CE} and V_{FG} are hardly different; the yield line of V_{CE} avoids the opening by passing point E of the intersection of diagonal reinforcement; V_{FG} is the lowest value among shear forces given by yield lines passing the center of the opening. However, the V_{AB} is the minimum for the specimen DB-1c as shown in Fig. C3.

In the same way, an yield line avoiding the diagonal reinforcement gives the solution V_{AC} for the specimens DB-2 as shown in Fig. C4; the following V_{EF} and V_{GH} were close each other, where the

yield line passed the opening and the other was extended from the beam end. As shown in Fig. C5, V_{CG} is the solution for the specimen DB-2e, where the yield line avoids the web opening. Regarding the specimen DB-3ce shown in Fig. C6, V_{DG} is the lowest and V_{EG} follows it, where both yield lines pass between the adjacent openings; V_{DG} is the upper bound solution of the shear capacity.
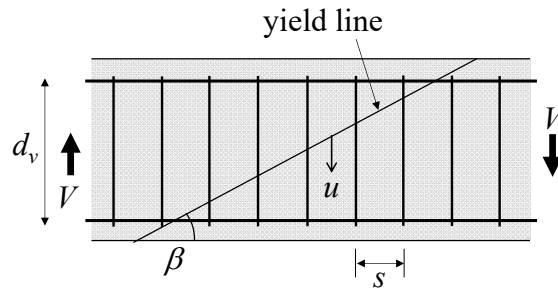

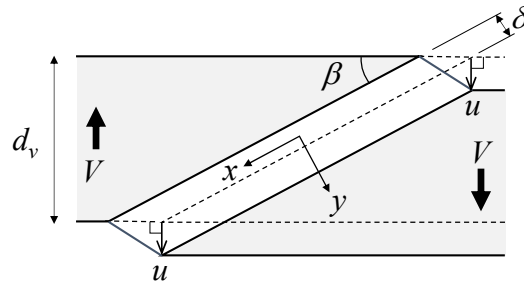*Fig. B1 – Shear failure model of RC beam*

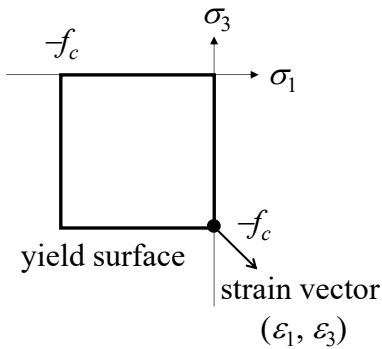*Fig. B2 – Strain field at yield line of concrete.*

Fig. B3 – Failure criterion of concrete.

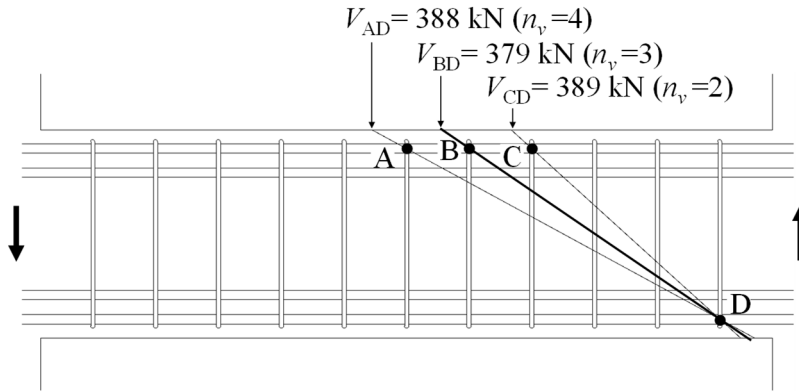V_{AD}= 388 kN (n_v=4)

V_{BD}= 379 kN (n_v=3)

V_{CD}= 389 kN (n_v=2)

Fig. C1 – Potential yield lines of DB-0. Note: 1 kN = 0.225 kip.

V_{EF}= 403 kN (n_v=0, A_d=71 mm$^2\times$ 8)

V_{GH}= 428 kN (n_v=2, A_d=71 mm$^2\times$ 8)

V_{AD}= 434 kN (n_v=2, A_d=0) V_{IJ}= 379 kN (n_v=3, A_d=0)

V_{AB}= 416 kN (n_v=3, A_d=0)
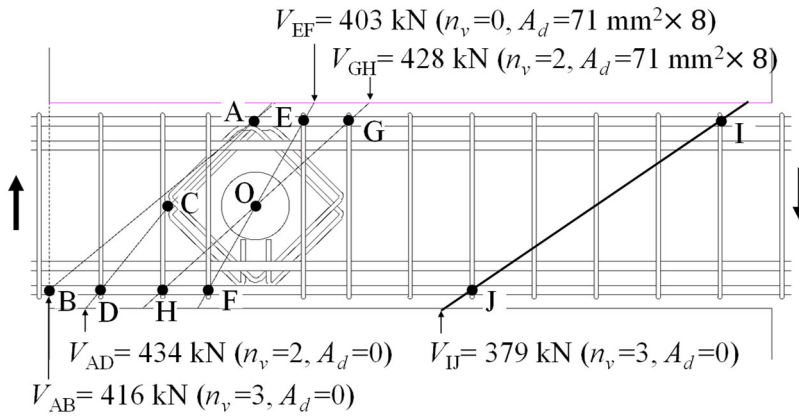
Fig. C2 – Potential yield lines of DB-1. Note: 1 kN = 0.225 kip; 1 mm^2 = 0.00155 in.^{2}.

V_{CE}= 448 kN (n_v=4, A_d=0)

V_{DE}= 454 kN (n_v=3, A_d=0)

V_{FG}= 447 kN (n_v=0, A_d=71 mm^2=71 mm$^2\times$ 8)

V_{AB}= 420 kN (n_v=3, A_d=0)
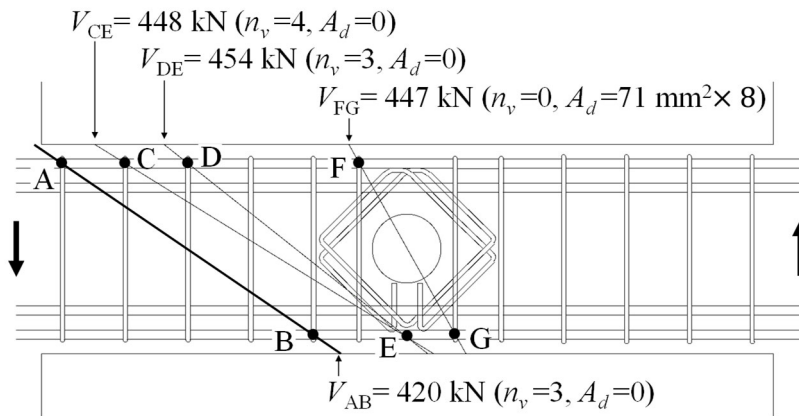
Fig. C3 – Potential yield lines of DB-1c. Note: 1 kN = 0.225 kip; 1 mm^2 = 0.00155 in.^{2}.

7

V_{GH}= 416 kN (n_v=3, A_d=0)

V_{EF}= 414 kN (n_v=0, A_d=71 mm²× 8)

A
E
G
B
C
D
F
H

V_{AD}= 434 kN (n_v=3, A_d=0)

V_{AC}= 409 kN (n_v=4, A_d=0)

V_{AB}= 421 kN (n_v=2, A_d=0)

Fig. C4 – Potential yield lines of DB-2. Note: 1 kN = 0.225 kip; 1 mm² = 0.00155 in.².

V_{AB}= 420 kN (n_v=3, A_d=0)

V_{CG}= 407 kN (n_v=3, A_d=0)

C
D
E
A
O
B
F
G
H

V_{EG}= 474 kN (n_v=1, A_d=50 mm²× 8)

V_{EH}= 448 kN (n_v=2, A_d=50 mm²× 8)

V_{DH}= 474 kN (n_v=3, A_d=50 mm²× 8)
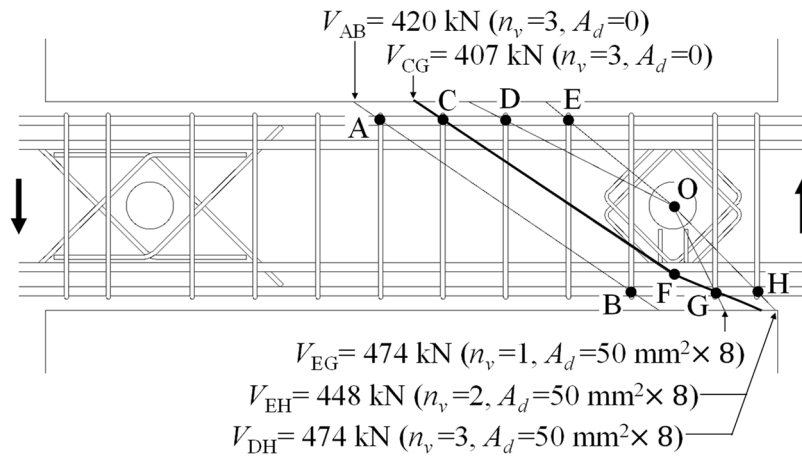
Fig. C5 – Potential yield lines of DB-2e. Note: 1 kN = 0.225 kip; 1 mm² = 0.00155 in.².

8

Fig. C6 – Potential yield lines of DB-3ce. Note: 1 kN = 0.225 kip; 1 mm² = 0.00155 in.².
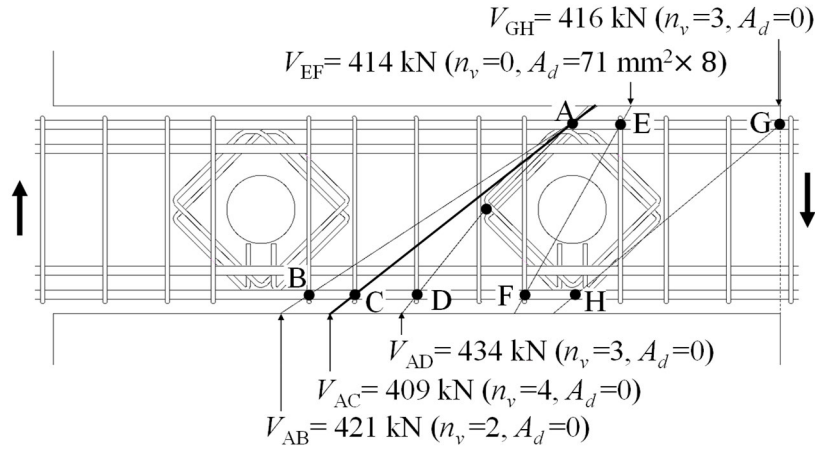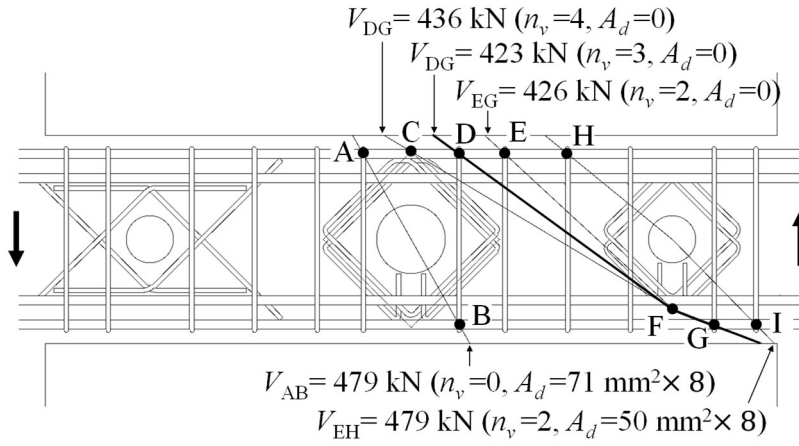
Fig. C6 labels:

V_{DG} = 436 kN (n_v=4, A_d=0)
V_{DG} = 423 kN (n_v=3, A_d=0)
V_{EG} = 426 kN (n_v=2, A_d=0)

V_{AB} = 479 kN (n_v=0, A_d=71 mm²× 8)
V_{EH} = 479 kN (n_v=2, A_d=50 mm²× 8)